

# Phenomenological model of vortex dynamics in arrays of Josephson junctions

T. P. Orlando,\* J. E. Mooij, and H. S. J. van der Zant

*Department of Applied Physics, Delft University of Technology, Delft, The Netherlands*

(Received 27 August 1990; revised manuscript received 5 December 1990)

A phenomenological model for arrays of Josephson junctions is developed in the continuum limit. This model gives a unified treatment of various types of behavior in arrays, such as charge solitons, vortices, collective modes, and the mass of the vortex. This model is then used to describe vortex dynamics when there is no pinning. We calculate the flux-flow resistivity due to vortex motion as well as consider the possibility of ballistic motion of vortices. We compare these results to the analogous situations in a conventional superconductor as well as for granular systems.

## I. INTRODUCTION

Arrays of Josephson junctions provide a convenient and controllable model system to study the effects of quantum mechanics on a macroscopic scale.<sup>1</sup> For such a system of Josephson junctions the phase of the order parameter and the number of superconducting electrons on each junction form a pair of conjugate dynamical variables. Although these variables are usually considered within the framework of quantum-mechanical dynamics,<sup>2,3</sup> the purpose of this paper is to develop the dynamics by considering these conjugate variables classically. In addition, the discrete nature of the array will not be considered in detail here when calculating physical properties. Hence, we will take the long-wavelength limit of the array so that the system can be considered as a continuum.

In Sec. II the energy storage in the array will be found first in the discrete array so that a well-defined transformation can be made to the continuum limit. The energy will be taken to be stored in three parts: in the Josephson junction, in the electric field, and in the magnetic field. With this form for the energy, one would usually have to develop a time-dependent Ginzburg-Landau theory to study the full dynamics of the array. Furthermore, the dissipation would need to be included by constructing an action that is nonlocal in time. Special cases of this theory have led to separate descriptions of several phenomena in the arrays, such as charge solitons, vortices, collective modes, and the mass of the vortex.<sup>2,3</sup> In this paper we choose a simplifying model, which replaces the time-dependent Ginzburg-Landau equation by a simpler Schrödinger-like equation and in which the dissipation is modeled in a phenomenological manner. We will refer to this approach as the macroscopic quantum model (MQM). The MQM is a good phenomenological model of a superconductor, and we explore a similar model for the array so that we can form a unified picture of its properties. We feel that such a unified model makes the interrelations among the various properties more manifest as well as that it provides a concise physical picture

that can shed light on the many implicit assumptions in the more general theories.

Therefore, in Sec. III the Lagrangian and the equations of motion for the array will be found within the MQM. The stationary solitonic solutions to these equations of motion are shown in Sec. IV to be of two types: charge-carrying solitons and flux-carrying vortices. Furthermore, we will mainly restrict our discussion of the arrays to the classical regime in which the Josephson energy of each junction is much larger than its charging energy. For such nonclassical arrays, the superconducting array can undergo a transition to an insulating phase. In practice, the normal-state resistance of each junction must be smaller than a kilohm to ensure a classical description.

In Sec. V a dispersion relation will be found in the classical dynamic limit and will be shown to be similar to the propagating plasma mode found in superconducting filaments by Mooij and Schön.<sup>4</sup> Also from the motion of vortex solutions, one finds that the vortex can be considered a particle with a mass that moves in a force-free environment. In Sec. VI the dissipation due to the flow of vortices is developed in the diffusive regime. Here an intuitive argument (along the lines of the Bardeen-Stephen model) is made for the effective flux-flow resistance and viscosity in the absence of pinning. Our intuitive argument further assumes that the moving vortex maintains its spatial integrity and does not excite other modes, such as spin waves or collective switching of the junctions. The Magnus-like force, which leads to a Hall resistance, is not considered, since estimates indicate that it is negligible. We find that the mean free path of the vortices is many lattice spacings. In contrast, for typical conventional superconductors the mean free path is much smaller than a coherence length. Because the lattice spacing plays the role of the coherence length, the vortices in the array are in a physically different regime than in a conventional superconductor. This long mean free path in the arrays means that if moving vortices are injected into a force-free regime, they can still be detected many lattice spacings away. Moreover, if the length of the array is

smaller than the mean free path, the vortices can move ballistically. In the Appendix we find the mass, energy, and force on a vortex when it is near a boundary and show that the presence of a boundary does not affect the motion of vortices if the array is wider than a few lattice constants.

## II. ENERGY STORAGE IN ARRAYS

Consider a two-dimensional array of identical Josephson junctions as shown in Fig. 1. In the absence of any applied currents, the energy  $W$  of the array is given by

$$W = W_J + W_E + W_B, \quad (1)$$

where  $W_J$  is the energy stored in the Josephson junctions,  $W_E$  is the energy stored in the electric field, and  $W_B$  is the energy stored in the magnetic field. Each of these energies will be considered in the discrete array and then the continuum limit will be taken.

The energy due to the Josephson junction itself is given by<sup>5</sup>

$$W_J = E_J \sum_{i,j} \{1 - \cos(\varphi[i+1, j] - \varphi[i, j])\} + E_J \sum_{i,j} \{1 - \cos(\varphi[i, j+1] - \varphi[i, j])\}. \quad (2)$$

Here  $E_J = \Phi_0 I_c / (2\pi)$  is the Josephson coupling energy, where  $\Phi_0$  is the flux quantum and  $I_c$  is the critical current of a single junction. The gauge-invariant phase  $\varphi[i, j]$  at the position  $[i, j]$  is

$$\varphi[i, j] = \theta[i, j] + (2\pi/\Phi_0) \int_{\text{ref}}^{[i,j]} \mathbf{A} \cdot d\mathbf{s}, \quad (3)$$

where  $\theta[i, j]$  is the phase of the macroscopic wave function (order parameter) at the site,  $\mathbf{A}$  is the magnetic vector potential, and  $d\mathbf{s}$  is a line element across the junction. In this paper we will only consider the array when the phase differences are small enough so that  $W_J$  can be expanded to lowest order in the phase differences to become

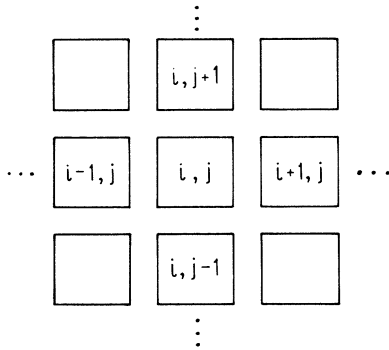


FIG. 1. A two-dimensional array of Josephson junctions on a square network with lattice constant  $p$ .

$$W_J \approx \frac{E_J}{2} \sum_{i,j} \{ (\varphi[i+1, j] - \varphi[i, j])^2 + (\varphi[i, j+1] - \varphi[i, j])^2 \}. \quad (4)$$

In the continuum limit it is convenient to define an energy density  $w_i$  so that the energy  $W_i = \int_{V_a} w_i dv$ , where  $V_a$  is the volume of the superconducting array. The “thickness” in the  $z$  direction of the two-dimensional array is taken to be  $d$ , and the superconducting properties do not vary in the  $z$  direction.<sup>6</sup> The Josephson energy density is then

$$w_J = \frac{E_J}{2d} \left( \nabla_{\perp} \theta + \frac{2\pi}{\Phi_0} \mathbf{A}_{\perp} \right)^2, \quad (5)$$

where the subscript  $\perp$  signifies that only the perpendicular component of the vector is used, that is, the component in the plane of the array.

The energy  $W_E$  stored in the array in a static electric field is just the electrical energy stored in the capacitive part of the network<sup>7</sup> and is given in terms of the scalar potential  $\phi[i, j]$  on each by

$$W_E = \frac{C_0}{2} \sum_{i,j} (\phi[i, j])^2 + \frac{C}{2} \sum_{i,j} (\phi[i+1, j] - \phi[i, j])^2 + \frac{C}{2} \sum_{i,j} (\phi[i, j+1] - \phi[i, j])^2, \quad (6)$$

where only nearest-neighbor contributions to the energy are considered. The capacitance to ground for each element is  $C_0$ . The capacitance between nearest neighbors is  $C$ , which consists not only of the geometrical capacitance but also a part due to quasiparticle tunneling.<sup>8,9</sup> In the continuum limit, in analogy to the Josephson energy, the electrical energy  $W_E$  can be written in terms of an energy density  $w_E$ , which is

$$w_E = \frac{C_0}{2dp^2} [\phi(x, y)]^2 + \frac{C}{2d} [\nabla_{\perp} \phi(x, y)]^2 \quad (7)$$

where the lattice spacing of the array is  $p$ . In most analyses of arrays,  $w_E$  is usually approximated by Eq. (7) even with time-varying fields. However, to study the full dynamics one must include the electrical energy due to the time-varying part of the magnetic vector potential. This means that  $\nabla_{\perp} \phi(x, y)$  must be replaced by  $\nabla_{\perp} \phi(x, y) + \partial \mathbf{A}_{\perp} / \partial t$  in the second term of Eq. (7). The first term of Eq. (7) can be left unchanged because any contribution due to the time variation of  $A_z$  will result in a current in the  $z$  direction (as seen in the next section), but currents are restricted in the plane of the array. Therefore,  $w_E$  is taken as

$$w_E = \frac{C_0}{2dp^2} [\phi(x, y)]^2 + \frac{C}{2d} \left( \nabla_{\perp} \phi(x, y) + \frac{\partial \mathbf{A}_{\perp}}{\partial t} \right)^2 \quad (8)$$

for the fully dynamical situations.

It is interesting to note that  $w_E$  can be thought of as

TABLE I. Comparison of the energy densities and equations of motion from the macroscopic quantum model for (1) the continuous 3D superconductor and (2) the array in the continuum limit.

	Continuous 3D superconductor	2D array in the continuum limit
Energy density	$w_K = \frac{\hbar^2 n_s^*}{2m^*} (\nabla\theta + \frac{2\pi}{\Phi_0} \mathbf{A})^2 + \frac{\hbar^2}{8m^* n_s^*} (\nabla n_s^*)^2$ $w_E = \frac{\epsilon_0}{2} \left( -\nabla\phi - \frac{\partial \mathbf{A}}{\partial t} \right)^2$ $w_B = \frac{1}{2\mu_0} (\nabla \times \mathbf{A})^2$	$w_J = \frac{E_c I_c}{2d} (\nabla_{\perp} \theta + \frac{2\pi}{\Phi_0} \mathbf{A}_{\perp})^2$ $w_E = \frac{C_0}{2dp^2} (\phi)^2 + \frac{C}{2d} (\nabla_{\perp} \phi)^2$ $w_B = \frac{1}{2\mu_0} (\nabla \times \mathbf{A})^2$
Phase-voltage relation	$\frac{\partial \theta}{\partial t} = \frac{2\pi}{\Phi_0} \phi - \frac{\hbar}{2m^*} (\nabla\theta + \frac{2\pi}{\Phi_0} \mathbf{A})^2$ $+ \frac{\hbar}{2m^* \sqrt{n_s^*}} (\nabla^2 \sqrt{n_s^*})$	$\frac{\partial \theta}{\partial t} = \frac{2\pi}{\Phi_0} \phi$
Continuity equation	$\frac{\partial Q}{\partial t} + \nabla \cdot \mathbf{J}_s = 0$ $Q = q^* (n_s^* - \tilde{n})$ $\mathbf{J}_s = -\frac{1}{\mu_0 \lambda_J^2} [\mathbf{A} + \frac{\Phi_0}{2\pi} \nabla\theta]$ $\mu_0 \lambda^2 = \frac{m^*}{n^* (q^*)^2}$	$\frac{\partial Q}{\partial t} + \nabla_{\perp} \cdot \mathbf{J}_s = 0$ $Q = q^* (n_s^* - \tilde{n})$ $\mathbf{J}_s = -\frac{1}{\mu_0 \lambda_J^2} [\mathbf{A} + \frac{\Phi_0}{2\pi} \nabla_{\perp} \theta]$ $\mu_0 \lambda_J^2 = \frac{\Phi_0^2 d}{4\pi^2 E_J}$
Amperes law	$\epsilon = \epsilon_0$	$\vec{\epsilon} = \begin{pmatrix} \frac{C}{d} & 0 & 0 \\ 0 & \frac{C}{d} & 0 \\ 0 & 0 & \frac{C_0 d}{p^2} \end{pmatrix}$
Gauss' law	$\mathbf{E} = -\nabla\phi - \frac{\partial \mathbf{A}}{\partial t}$ $Q = -\epsilon_0 \nabla \cdot (\nabla\phi + \frac{\partial \mathbf{A}}{\partial t})$	$\mathbf{E}' = -\frac{\phi}{d} \mathbf{i}_z - (\nabla_{\perp} \phi + \frac{\partial \mathbf{A}_{\perp}}{\partial t})$ $Q = \frac{C_0}{dp^2} \phi - \frac{C}{d} \nabla_{\perp} \cdot (\nabla_{\perp} \phi + \frac{\partial \mathbf{A}_{\perp}}{\partial t})$

the energy due to an electric field  $\mathbf{E}'$  in an anisotropic dielectric medium. The electric field is

$$\mathbf{E}' = -\frac{\phi}{d} \mathbf{i}_z - \left( \nabla_{\perp} \phi(x, y) + \frac{\partial \mathbf{A}_{\perp}}{\partial t} \right). \quad (9)$$

The energy density, which is equivalent to Eq. (8), can be written as  $w_E = \mathbf{E}' \cdot \vec{\epsilon} \cdot \mathbf{E}'/2$  where  $\vec{\epsilon}$  is the effective dielectric tensor and is listed in Table I.

The third and final way in which the energy is stored is in the magnetic field. The energy density  $w_B$  due to the magnetic field is given by

$$w_B = \mathbf{B}^2/(2\mu_0) = (\nabla \times \mathbf{A})^2/(2\mu_0) \quad (10)$$

where  $\mathbf{B}$  is the magnetic flux density.

### III. EQUATIONS OF MOTION

Having found the energy densities, we can now find the dynamic equations of motion by appealing to the MQM, which models the superconductor as a collisionless electron gas in a positive background. Although the MQM model is not the full theory of superconductivity,<sup>10</sup> it does explain most of the basic equations of a superconductor such as the London equations, flux quantization, and the Josephson equations.<sup>11–13</sup> For example, in the continuous three-dimensional (3D) superconductor, the MQM describe the superconductor by a macroscopic order parameter  $\Psi(\mathbf{r}, t)$ , which is of the form  $\Psi(\mathbf{r}, t) = \sqrt{n_s^*(\mathbf{r}, t)} \exp[i\theta(\mathbf{r}, t)]$ , where  $n_s^*$  is the density of superconducting electron pairs.

The equations of motion describing the fields and currents follow from the Lagrangian density  $\mathcal{L}$  which can be written as<sup>14,15</sup>

$$\mathcal{L} = -\hbar n_s^* \frac{\partial \theta}{\partial t} - w_K + w_E - w_B - (n_s^* - \tilde{n}) q^* \phi. \quad (11)$$

Here  $w_K$  is the kinetic energy density, and  $\tilde{n}$  is the background charge density needed to make the array overall neutral. The corresponding energy densities and resulting equations of motion for continuous superconductor are listed in Table I.

In applying the MQM to the continuum limit of the array, we assume that the equations of motion follow from its Lagrangian density,<sup>15</sup> which is the same form as Eq. (11) but with  $w_J$  replacing  $w_K$ . The corresponding energy densities are also listed in Table I.

The Euler-Lagrange equation for the density  $n_s^*$  gives the first equation of motion for the 2D array as

$$\frac{\partial}{\partial t} \theta(\mathbf{r}, t) = \frac{2\pi}{\Phi_0} \phi. \quad (12)$$

When written in terms of the gauge-invariant phase  $\varphi$ , this is just the Josephson phase-voltage relationship, namely,  $\partial\varphi/\partial t = (2\pi/\Phi_0)v$ , where  $v$  is the voltage. A comparison of this equation of motion with its analogous one for the continuous 3D system reveals that the array has fewer terms. This is because  $w_J$  does not depend on the density, since the critical current  $I_c$  is considered fixed.

The Euler-Lagrange equation for the gauge-invariant phase  $\varphi$  gives the continuity equation for the array as

$$\frac{\partial Q}{\partial t} + \nabla_{\perp} \cdot \mathbf{J}_s = 0. \quad (13)$$

Here  $Q = q^*(n_s^* - \tilde{n})$  is the excess charge. The current density is assumed to be only in the plane of the array and is given by

$$\mathbf{J}_s(\mathbf{r}, t) = -\frac{1}{\mu_0 \lambda_J^2} \left( \mathbf{A}(\mathbf{r}, t) + \frac{\Phi_0}{2\pi} \nabla_{\perp} \theta(\mathbf{r}, t) \right), \quad (14)$$

where  $\lambda_J = \sqrt{\Phi_0^2 d / (4\mu_0 \pi^2 E_J)}$  is the usual Josephson penetration depth.

The third equation of motion for the array, Ampere's law, follows from the Euler-Lagrange equation for  $\mathbf{A}$  and is

$$\nabla \times \mathbf{B} = \mu_0 \mathbf{J}_s + \mu_0 \frac{\partial}{\partial t} (\vec{\epsilon} \mathbf{E}'). \quad (15)$$

The Euler-Lagrange equation for the scalar potential  $\phi$  gives the fourth and final equation of motion as

$$Q = \frac{C_0}{dp^2} \phi - \frac{C}{d} \nabla_{\perp} \cdot \left( \nabla_{\perp} \phi + \frac{\partial \mathbf{A}_{\perp}}{\partial t} \right). \quad (16)$$

This can be seen to be Gauss's electric law by using the integral form of Gauss's law with a dielectric tensor.

Equations (12), (13), (15), and (16) are the four equations of motion for the array, and they are listed in Table I. In the following sections, some solutions to these equations will be found.

#### IV. STATIONARY SOLITONIC SOLUTIONS

Two types of stationary singular solutions can be found for the equations of motion for the array when all the measurable fields are independent of time. One solution carries electric charge and the other carries flux.

In one-dimensional arrays of capacitors, charge-carrying solitonic solutions have been found.<sup>16</sup> Recently, such solutions have been found in 2D systems.<sup>17,18</sup> These 2D solutions follow from the time-independent form of Gauss's law for the array, which from Eq. (16) is of the form of a scalar Helmholtz equation, namely,

$$Q = \frac{C_0}{dp^2} \phi - \frac{C}{d} \nabla_{\perp}^2 \phi. \quad (17)$$

When the excess charge is a point charge so that  $Q = -(e/d)\delta_2(\mathbf{r})$ , ( $\mathbf{r}$  is the radius in polar coordinates), the resulting potential in the plane of the array is given by

$$\phi = -\frac{e}{2\pi C} K_0(r/r_0), \quad (18)$$

where  $K_0$  is the modified Bessel function of order zero. The decay length of the potential is  $r_0 = p\sqrt{C/C_0}$ . Hence the field due to the point charge is confined mostly to a region of  $r_0$  about the charge. This means that the charge solitonic solution has no net charge associated with it in an infinite system because the array of junctions along with the capacitance to ground completely

screens out the point charge at large distances.

It has been assumed that the electric field is confined to the the plane of the array in deriving the charge solitonic solution. This is a good approximation for arrays of small Josephson junctions.<sup>17</sup> However, in granular films the electric field can be in the free space outside of the film, where the potential satisfies Laplace's equation. In this case the solution to such a problem has been found by Pearl<sup>19</sup> and can be approximated by

$$\phi = -\frac{e}{2\pi C} \ln \left( \frac{r}{1 + r/2r_{\perp}} \right) \quad (19)$$

where  $r_{\perp} = r_0^2/d$  is the decay length. Usually  $r_{\perp} \gg r_0$  so that in such granular systems the charge solitonic solutions decay with a much greater length scale.

Just as the Maxwell equation for the charge led to a charge soliton, the Maxwell equation for the current (Ampere's law) leads to a flux soliton. For stationary fields, Ampere's law [Eq. (15)] becomes

$$\nabla \times \mathbf{B} = \mu_0 \mathbf{J}_s, \quad (20)$$

and the current density is still given by Eq. (14). Quantized vortices are described near their core by a phase given by<sup>11</sup>

$$\theta = \tan^{-1} y/x. \quad (21)$$

(For distances larger than the penetration depth of the superconductor, the phase decays exponentially.) Equations (14), (20), and (21) can be combined to show that the magnetic flux density in the plane of the array satisfies

$$\nabla^2 \mathbf{B} - \frac{1}{\lambda_J^2} \mathbf{B} = -\frac{\Phi_0}{\lambda_J^2} \delta_2(\mathbf{r}) \mathbf{i}_z. \quad (22)$$

In the free space outside of the array, the magnetic field again satisfies Laplace's equation. Again Pearl<sup>19</sup> has found that the magnetic field in the plane of the array can be approximated by

$$B_z^p = \frac{\Phi_0}{2\pi \lambda_J^2} \ln \left( \frac{r}{1 + r/2\lambda_{\perp}} \right). \quad (23)$$

Here the effective penetration depth for the flux is  $\lambda_{\perp} = \lambda_J^2/d$ .

#### V. DYNAMICS

Eckern and Schmid<sup>3</sup> have found the dispersion relation for collective modes related to the electric potential and, hence, related to the charge solitons, for the array in the continuum limit. These modes exist as long as the magnetic field does not contribute greatly to their properties. On the other hand, when the magnetic field is applied perpendicular to the array, vortices form in the array. Furthermore, these vortices will move under the influence of a driving current. It has been shown that these moving vortices can be described as a particle with a mass  $M_v$ .<sup>2,3</sup> From the equations of motion in Sec. III,

we will first find the dispersion relation for the scalar potential and then discuss the motion of a vortex.

A classical dispersion relation can be found by combining the time derivative of the continuity equation [Eq. (13)] with the Josephson phase-voltage relation [Eq. (12)] and Gauss's electric law [Eq. (16)]. If the time rate of change of  $\mathbf{A}$  is small enough, then this procedure reduces to the wave equation found by Eckern and Schmid,<sup>3</sup> namely,

$$-\frac{4\pi^2 E_J}{\Phi_0^2} \nabla_{\perp}^2 \phi + \frac{C_0}{p^2} \frac{\partial^2 \phi}{\partial t^2} - C \nabla_{\perp}^2 \frac{\partial^2 \phi}{\partial t^2} = 0. \quad (24)$$

This equation results in the following dispersion relation:

$$\omega^2 = \frac{c_s^2 k^2}{1 + (c_s k / \Omega)^2}, \quad (25)$$

where  $c_s^2 = (2\pi p)^2 E_J / (C_0 \Phi_0^2)$  and  $\Omega^2 = (2\pi)^2 E_J / (C \Phi_0^2)$ . For low values of  $k$  (long wavelengths), the dispersion relation is acousticlike with a velocity of propagation  $c_s$ . For shorter wavelengths the dispersion relation saturates at the Josephson plasma frequency  $\Omega$ . An approximate crossover in  $k$  occurs at  $r_0^{-1}$ ; hence, when the acousticlike mode has a wavelength shorter than the screening length  $r_0$  of the charge soliton, the acoustic mode can no longer propagate. At these shorter wavelengths the array undergoes a collective oscillation where each junction is oscillating at its Josephson plasma frequency.

The acoustic mode is the two dimensional version of the propagating plasma mode in thin superconducting filaments that was predicted by Mooij and Schön<sup>4</sup> and by Kulik.<sup>20</sup> In fact, if the analysis done in this section is done for a one-dimensional superconductor with the appropriate capacitance to ground, then one gets exactly the velocity of the one-dimensional mode given by Mooij and Schön. Consequently, this also means that a linear array of Josephson junctions should give rise to this mode so that the propagating mode for the one-dimensional charge solitons<sup>16</sup> is the Mooij-Schön mode. The reason the propagating plasma mode survives in our two-dimensional array is that the charge of the soliton is completely screened out, thereby allowing for the formation of an acoustic branch in the dispersion relation.

We now find a wavelike equation that describes the magnetic properties of the array, in analogy to Eq. (24), which describes the electrical properties of the array. This equation can be written in terms of  $\mathbf{B}$  by combining the curl of the superconducting current density [Eq. (14)] with Ampere's law [Eq. (15)]. Then by using the definition of  $\mathbf{E}'$  [Eq. (9)] and the phase-voltage relation [Eq. (12)], we find

$$\begin{aligned} \nabla^2 \mathbf{B} - \frac{1}{\lambda_J^2} \mathbf{B} - \frac{1}{\bar{c}^2} \frac{\partial^2 \mathbf{B}}{\partial t^2} \\ = \frac{\Phi_0}{2\pi \lambda_J^2} \nabla \times \nabla \theta + \frac{\Phi_0 C_0 \mu_0}{2\pi p^2} \nabla \times \left( \frac{\partial^2 \theta}{\partial t^2} \mathbf{i}_z \right). \end{aligned} \quad (26)$$

Here  $\bar{c} = \sqrt{d/(\mu_0 C)} = \lambda_J \Omega$  is a velocity of propagation.

A stationary vortex at the origin has a phase near its core  $\theta$  given by Eq. (21). When this is inserted into the time-independent form of Eq. (26) one obtains the usual equation of a stationary vortex [Eq. (22)], which gives the flux density  $B_z^p(r/\lambda_J)$  in Eq. (23).

To find the magnetic flux density for a moving vortex, we assume that the moving vortex maintains the same phase distribution of Eq. (21) as it moves with a constant velocity  $\mathbf{u}$ . Therefore, if the center of the vortex is at  $\mathbf{r}_0 = (u_x t, u_y t)$ , then the phase of the moving vortex near its center is

$$\theta(t) = \tan^{-1} \frac{y - u_y t}{x - u_x t}. \quad (27)$$

If we assume that the resulting  $\mathbf{B}$  is only in the  $z$  direction, then substitution of  $\theta(t)$  into the Eq. (26) gives

$$\begin{aligned} \nabla^2 B_z(\mathbf{r}, t) - \frac{1}{\lambda_J^2} B_z(\mathbf{r}, t) - \frac{1}{\bar{c}^2} \frac{\partial^2 B_z(\mathbf{r}, t)}{\partial t^2} \\ = -\frac{\Phi_0}{\lambda_J^2} \delta_2(\mathbf{r} - \mathbf{u}t) \mathbf{i}_z, \end{aligned} \quad (28)$$

which the time-dependent form of Eq. (22). The time-dependent solution to Eq. (28) for a vortex is then

$$B_z(\mathbf{r}, t) = B_z^p(|\mathbf{r} - \mathbf{u}t|/\lambda_{\text{eff}}), \quad (29)$$

where  $\lambda_{\text{eff}} = \lambda_J \sqrt{1 - (u/\bar{c})^2}$ . In other words, the moving vortex has the same magnet flux profile as a stationary vortex that moves, but it has an effective penetration depth that undergoes a Lorentz transformation.<sup>21</sup> In this paper we will assume  $u \ll \bar{c}$ .

To understand the full dynamics of a moving vortex, it is necessary to find not only its magnetic flux, but also the electric field that it generates due to its motion. It has been shown that the effect of the electric field is equivalent to considering the vortex as a particle of mass  $M_v$ .<sup>2,3</sup>

Before giving a detailed calculation of this mass, consider the following qualitative argument. If the vortex moves with a speed  $u$ , then the phase will change by  $\pi$  as the center of the vortex crosses a lattice parameter in the time  $u/p$ . Therefore, we expect that  $\delta\varphi/\delta t \approx \pi u/p$ . From the phase-voltage relation [Eq. (12)], we can estimate that an average voltage  $\langle v \rangle$  appears across the array that is given by  $\langle v \rangle \approx \Phi_0 u/(2p)$ . Now the electric energy  $W_E$  is stored in the capacitors, so that for  $C \gg C_0$ ,  $W_E \approx \sum_{i,j} C (\phi_{i,j})^2 / 2$  where the sum is over all the capacitors and  $\phi_{i,j}$  is the potential across the capacitors. If we estimate the sum of the squares of the potentials as proportional to the square of the average voltage, we find with a proportionality constant of  $\gamma$  that  $W_E \approx \gamma C \Phi_0^2 u^2 / (8p^2)$ . Hence we see that  $W_E$  acts like a kinetic energy term with the mass of the vortex given by  $M_v \approx \gamma C \Phi_0^2 / (4p^2)$ . To be consistent with the value of the mass found by Eckern and Schmid,<sup>3</sup> namely,

$$M_v = C \Phi_0^2 / (2p^2), \quad (30)$$

we must demand that  $\gamma = 2$ .

To see in more detail how the vortex develops a mass, the energy  $W$  is found for a moving vortex when its velocity is such that  $u \ll \bar{c}$ . It is assumed that the moving vortex maintains the same phase distribution of Eq. (21) as it moves. Therefore, let the center of the vortex be at  $(x_0(t), y_0(t))$ , so that the phase of the moving vortex near its center is

$$\theta = \tan^{-1} \frac{y - y_0(t)}{x - x_0(t)}. \quad (31)$$

From Eqs. (5) and (10) we find that for a moving vortex the energy stored in  $W_J$  and  $W_B$  is just the energy stored in a stationary vortex,<sup>19</sup>  $\mathcal{E}_V = [\Phi_0^2/(2\pi\lambda_\perp)] \ln(2\lambda_\perp/\xi)$ . Here  $\xi$  is a cutoff length for the vortex. For a vortex in a continuous superconductor,  $\xi$  is just the core radius. By carefully considering the array-to-continuum limit, it has been shown<sup>3</sup> that for the array  $\xi = p/\sqrt{2\pi}$ . Because  $\mathcal{E}_v$  does not depend on the velocity of the vortex, it is a constant offset to the energy, which does not contribute to describing its dynamics.

The dynamical contribution to the energy of the moving vortex in the infinite array is then determined only by  $w_E$ . The moving vortex generates a scalar electric potential through the Josephson phase-voltage relation of Eq. (12) and this potential depends explicitly on the velocity  $(\dot{x}_0, \dot{y}_0)$  of the moving vortex. (The contribution from the time rate of change of the vector potential is again assumed small and is neglected.) When  $w_E$  is integrated over all space, the integral must be cut off not only at  $\xi$  for short distances but also at  $\lambda_\perp$  for large distances because of the approximate solution of the phase used. This integration gives  $W_E = M_v (\dot{x}_0^2 + \dot{y}_0^2)/2$ . Here  $M_v$  is the effective mass of the vortex, and  $M_v = m_0 + M_1$ , where  $m_0 = [\Phi_0^2 C_0/(2\pi p^2)] \ln(\lambda_\perp/\xi)$  and  $M_1 = \Phi_0^2 C/(2p^2)$ . Because  $C \gg C_0$ , the contribution of  $m_0$  to the total mass is negligible so that  $M_v \approx M_1$ . Hence, the energy stored in the moving vortex is just the energy due to a particle of mass  $M_v$  moving in a force-free environment. For  $C \approx 10^{-15}$  F and  $p \approx 1 \mu\text{m}$ , then  $M_v \approx 0.01 m_e$ , where  $m_e$  is the mass of the electron. This mass can change if the vortex is near a boundary. However, in the Appendix we show that these boundary effects are negligible if the vortex is a few lattice spacings away from the boundary.<sup>22</sup>

## VI. TRANSPORT OF VORTICES

In the presence of a magnetic field  $\mathbf{B}$  perpendicular to the array, vortices form. In the continuum limit these vortices form an array with a density  $n_v = B/\Phi_0$ . If an applied current is put through the array, these vortices will move and dissipate power. A phenomenological method is proposed to model the flux flow in the array, analogous to the Bardeen-Stephen<sup>23</sup> model for the 3D system. [In this model we assume that the spatial structure of the vortex given by Eq. (27) is stable and that the moving vortex does not excite other dissipative modes in the system.] In the array, just as in the 3D system, it is

necessary to look at the power dissipation on the length scale of  $\xi$ . Therefore, it is necessary to return to the discrete array to calculate the power loss due to the vortex motion.

Consider the discrete array shown in Fig. 2 in which a current  $i$  is put through the array. The array is taken to have a period  $p$ , and to have a length in the  $x$  direction of  $L_x = Np$  and in the  $y$  direction of  $L_y = Mp$ . The current  $i$  is sent in the  $y$  direction and is passed through the array from bulk superconducting contacts. The magnetic field is assumed greater than  $H_{c1}$ , so that the average distance between vortices in the array is much less than  $\lambda_J$ . This number of vortices assures that the current will flow, on the average, uniformly down the array. Therefore, on the average, a current of  $I = i/N$  flows down each column of the array. Under these conditions, the vortices will experience a Lorentz-like force that will move the vortices in the  $x$  direction. In this section the array is assumed to be a viscous medium, which causes the vortices to move with a constant velocity  $\tilde{u}_x$ . More specifically, we model the force on each vortex by the usual flux flow model so that<sup>11</sup>

$$M_v \frac{d\tilde{u}_x}{dt} + \eta \tilde{u}_x = \frac{\Phi_0 i}{L_x}. \quad (32)$$

Here  $\eta$  the viscosity of the medium to flux flow and is a phenomenological parameter that will be determined.

For the moving vortices Faraday's law demands that a voltage  $v$  appear across the array, in the direction of the current flow, such that

$$v = \Phi_0 \tilde{u}_x L_y n_v. \quad (33)$$

The power  $P$  dissipated by the current supply is then

$$P = iv = i\Phi_0 \tilde{u}_x L_y n_v. \quad (34)$$

These two global considerations, however, do not determine what  $\tilde{u}_x$  is. Nevertheless, the global requirement for power loss can be connected to the local description of power loss by noting that the equation of motion of a single vortex demands that each vortex dissipates a power

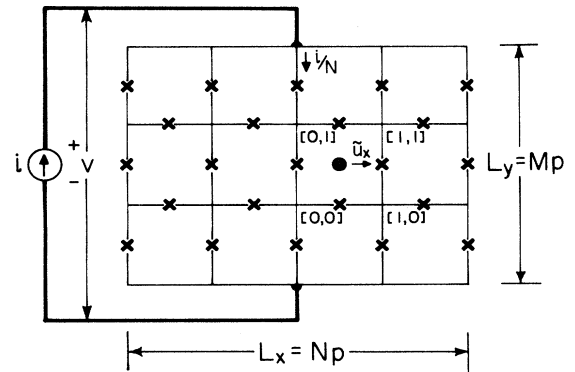


FIG. 2. The array with a current  $i$  flowing. A vortex is shown at the position  $[1/2, 1/2]$ .

$P_J$  due to the viscous medium. If the vortex moves with the steady-state velocity  $\tilde{u}_x$ , then

$$P_J = \eta \tilde{u}_x^2. \quad (35)$$

Assuming that each vortex dissipates power independently, then the total power dissipation is

$$P = P_J n_v L_x L_y. \quad (36)$$

By considering the origin of the power loss in each junction, we can then determine the parameters, such as  $\eta$ ,  $\tilde{u}_x$ , and  $P$ .

The origin of  $P_J$  is first given by a qualitative argument. The voltage generated by the moving vortex across the junction at  $[i, j]$  is denoted as  $\phi_{i,j}$ . Since each junction has some resistance  $R_{i,j}$ , the power loss due to each junction is just the sum of the resistive losses, namely,  $P_J = \sum_{i,j} \phi_{i,j}^2 R_{i,j}^{-1}$ . If we assume that each junction is characterized by the same average effective resistance  $R_A$ , then  $P_J \approx R_A^{-1} \sum_{i,j} \phi_{i,j}^2$ . As in the argument for the mass, we again estimate the sum of the squares of all the voltages as proportional to the square of the average voltage  $\langle v \rangle$ . Consequently,

$$P_J \approx \gamma \Phi_0^2 \tilde{u}_x^2 / (4R_A p^2) = \Phi_0^2 \tilde{u}_x^2 / (2R_A p^2), \quad (37)$$

where  $\gamma = 2$  as used before. Comparison of this with Eq. (35) gives

$$\eta \approx \Phi_0^2 / (2R_A p^2) \approx M_v / (R_A C). \quad (38)$$

Having found the viscosity in terms of local parameters, we can now find the velocity and also the voltage generated by the vortices. The steady-state velocity can be written in terms of  $\eta$  by using Eq. (32), namely,

$$\tilde{u}_x = i\Phi_0 / (\eta L_x) \approx 2iR_A p^2 / (\Phi_0 L_x). \quad (39)$$

The voltage due to the moving vortices is given by Eq. (33) which can be characterized by an equivalent flux flow resistance per square,  $R_{\text{ff}}^0$ ; namely,

$$R_{\text{ff}}^0 = 2Bp^2 R_A / \Phi_0. \quad (40)$$

$R_{\text{ff}}^0$  is similar to the flux flow resistance in a continuous 3D system<sup>23</sup> and in a long Josephson junction.<sup>24,21</sup>

To justify the qualitative model, we now give a more detailed calculation of the voltage and losses due to vortex motion. Consider the voltage generated across each junction as the vortex moves. Let the junction have the  $y$  coordinate of  $1/2$  as shown in Fig. 2. Then in analogy to Eq. (31) for the continuum limit, the phase across each junction due to the moving vortex is given by

$$\theta[i, j] = \tan^{-1} \left( \frac{j - 1/2}{i - \tilde{u}_x t / p} \right). \quad (41)$$

For the Josephson phase-voltage relation of Eq. (12) gives the potential as

$$\phi[i, j] = -\frac{\Phi_0 \tilde{u}_x}{2\pi p} \frac{j - \frac{1}{2}}{(i - \tilde{u}_x t / p)^2 + (j - \frac{1}{2})^2}. \quad (42)$$

The power loss through each junction is just this potential times the current  $I$  through the junction. The sum of all these power losses is the same as that given by in Eq. (34). Note, however, that the largest voltage drop  $\delta v$  occurs across the junction nearest to the core of the vortex and over which the core transverses.<sup>25</sup> We will call such a junction the ‘‘core’’ junction.

At time  $t = 0$  the core junction is that junction between the nodes  $[0, 1]$  and  $[0, 0]$  in Fig. 2. Consider the voltage  $\delta v = \phi[0, 0] - \phi[0, 1]$  across this junction in the direction of the current flow. With Eq. (42), this voltage difference can be seen to have a Lorentzian line shape given by

$$\delta v = \Phi_0 \frac{p}{2\pi \tilde{u}_x} \frac{1}{t^2 + p^2 / (2\tilde{u}_x)^2}. \quad (43)$$

This voltage has a full width at half maximum (FWHM) of  $p/\tilde{u}_x$ , which is the time it takes the vortex to cross one cell. The maximum voltage across this junction occurs at  $t = 0$  and is given by  $\delta v' = 2\Phi_0 \tilde{u}_x / (\pi p)$ . However, for the Lorentzian line shape, the average voltage  $\langle \delta v \rangle$  that occurs across all the junctions as the vortex moves across the sample is just the total flux divided by the FWHM time, that is,  $\langle \delta v \rangle = \Phi_0 \tilde{u}_x / p$ . Hence,  $\langle \delta v \rangle$  is nearly equal to  $\delta v'$ , so that the average power dissipation is nearly equal to the maximum power dissipation, showing that most of the power dissipated across a junction occurs when it is a core junction.

The fundamental assumption of our phenomenological model of the flux flow is that the power dissipated is assumed to scale with the average power dissipated across the core junctions. Each of these junctions dissipates an average power of  $I \langle \delta v \rangle$ . Therefore,  $P$  is proportional to the power loss of each core junction times the total number of vortices, namely,  $P = \alpha i \langle \delta v \rangle n_v L_x L_y / N$ , where  $\alpha$  is a constant of proportionality. Putting  $\langle \delta v \rangle$  into this equation gives that  $P = \alpha i \Phi_0 \tilde{u}_x n_v L_y$ . Comparison with Eq. (34) shows that  $\alpha = 1$ . Therefore, if  $P_J$  is the power dissipated across one of the core junctions, then one has the intuitive result that  $P = P_J n_v L_x L_y$ . For the moment  $P_J$  will be taken as a phenomenological parameter that is known for a single junction. A comparison with Eq. (34) determines the velocity of the vortex as  $\tilde{u}_x = P_J L_x / (i \Phi_0)$ . This velocity gives a voltage according to Eq. (33), which is equivalent to a flux flow resistance per square

$$R_{\text{ff}}^0 = Bp^2 R_e / \Phi_0, \quad (44)$$

where

$$R_e = P_J / I^2. \quad (45)$$

Here  $R_e$  is the effective resistance that describes the power loss of a single junction.

Note that in our argument, we have assumed that the power loss is just  $I \langle v \rangle$ ; that is, just the product of the average current and the average voltage. More accurately, we should calculate the average of the instantaneous power,  $iv$ , for each junction, and then average this

quantity over the time it takes the vortex to cross the sample. The assumption is analogous to the approximation used in Eq. (37), where we estimated that the sum of the squares of the all the voltages is proportional to the square of the average voltage. Therefore, we expect the same proportionality constant of  $\gamma = 2$ , so that for a resistively shunted junction, we have  $R_e = 2R_A$ . In a similar manner, the viscosity can now be found by using Eq. (39); therefore, we again find a result nearly identical to the more qualitative argument,  $\eta = \Phi_0^2/(p^2 R_e)$ . In fact, most of the results of the qualitative argument can be made identical to the more detailed results by replacing  $R_e$  with  $2R_A$ .

The effective resistance has the following interpretation. Recall that  $P_J$  is the power loss in a single junction. Because the moving vortex determines the potential drop, then  $P_J$  is the power dissipated in a single junction when it is voltage biased and a current  $I$  is flowing. Consequently,  $R_e$  is the resistance of a single junction when it is voltage biased. We note this model of the effective resistance assumes that the moving vortices do not create additional quasiparticles. However, Eckern and Schmid have suggested that the additional quasiparticles are indeed created, especially when the vortex creates a voltage near the gap voltage.<sup>3</sup> This means that the effective resistance, especially in the subgap regime, can be smaller than given by our model.

Now that all the parameters in the equation of motion for the vortex [Eq. (32)] have been determined, the time-dependent motion of a vortex can be discussed. Consider the case of a current  $i$  driving an array of vortices in a magnetic field as in Fig. 2. In steady state the vortices attain a terminal velocity of  $\tilde{u}_x$ . If the current is suddenly turned off, then the vortices will continue to move but their velocity will decay exponentially in time as  $u_x(t) = \tilde{u}_x \exp(-t/\tau_v)$ , where  $\tau_v = M_v/\eta = R_e C/2$ . With this velocity the vortices will travel a distance  $x_f$  before coming to rest, where

$$x_f = \tilde{u}_x \tau_v = \frac{1}{4\pi} p \beta_c(R_e) \frac{I}{I_c}, \quad (46)$$

and  $\beta_c(R) = 2\pi I_c R^2 C/\Phi_0$  is the Stewart-McCumber parameter. This calculation for  $x_f$  is analogous to the calculation of the mean free path for electrons in the normal state, so that  $x_f$  is the mean free path for the vortices.

For  $\beta_c$  in the range of 1000 for an array and the current a fraction (say 0.1) of the critical current, then the  $x_f$  is about 10 lattice spacings (or equivalently, coherence lengths). This distance should be contrasted with that for a 3D continuous superconductor, where  $x_f$  is of the order of  $10^{-5}$  of a coherence length. To understand why a vortex in an array goes nearly a million times further (measured in coherence lengths) than a vortex in a usual 3D superconductor, consider the velocity and relaxation times of each system. If a vortex is driven by the maximum applied current,  $I_c$  in an array, and the depairing current density in a 3D system, then the vortex will go a coherence length in both systems in the time of or-

der of  $\hbar/\Delta$ . For lower driving currents, the vortex will go slower, but its speed will still be of the same order of magnitude. Hence, we see that in both systems the speed of the vortex is about the same. The difference in the mean free paths must then be due to the different relaxation times. In the array, we found this to be of the order of the  $RC$  time constant  $\tau_{RC}$  for the junction. For a junction of 1 k $\Omega$  and 10 fF, then  $\tau_{RC} \approx 10^{-11}$  s. For a 3D superconductor the corresponding time constant is  $\tau_e = \epsilon_0/\sigma_0$ , the charge relaxation time. For a granular superconductor with a resistivity of about 100  $\mu\Omega$  cm, then  $\tau_e \approx 10^{-17}$  s. Hence, the difference in the mean free paths comes about from the vastly different relaxation times for the vortices in the two systems. Therefore, vortices in an array can have  $x_f > \xi$ , whereas conventional superconductors usually have  $x_f \ll \xi$ , and thus arrays open the possibility of studying vortex motion in a different physical regime.

Because  $R_e$  is a nonlinear function of  $I$ , it is possible to have the vortices go much further than  $x_f$ . To obtain the longest decay time, one needs to have the current  $i$  as small as possible. One way to achieve both of these criteria is to drive the vortices in one region to the maximum velocity and then inject them into a region where there is no current and no magnetic field. In this second region the vortex velocity will decay with a time constant that is much longer than in the first region and so it will go much further. Specifically, if the effective resistance per square in the first region is  $R_I$  and in the second region is  $R_{II}$ , then  $R_{II}$  can be much larger than  $R_I$ . In this case the vortex will go a distance  $l_f$  before coming to rest, namely,

$$l_f = u_x^I \tau_v^{II} = \frac{1}{4\pi} p \beta_c(R_I) \frac{I}{I_c} \left( \frac{R_{II}}{R_I} \right). \quad (47)$$

A summary of the parameters for a vortex is given in Table II along with the parameters for the continuous 3D superconductor for comparison.

## VII. SUMMARY

In this section we discuss some of the assumptions of our model that will effect the motion of vortices and summarize the main results of this paper.

The first important assumption is that the arrays are classical, such that  $E_J > E_C$ . The second important assumption is that the vortex solution is not only stable but also that it preserves its integrity as it moves. It is possible that a moving vortex will excite other dissipative modes in the array that could effect the value of the flux flow resistance. Furthermore, experiments show that for high driving currents the array goes from flux flow behavior to modes that correspond to the switching of rows.<sup>27</sup> In this paper we have assumed that the driving current is low enough so that this switching is not important. However, no theoretical criterion has yet been developed to determine when this behavior changes, but experiments suggest that the higher the  $\beta_c$  the lower



TABLE II. Comparison of the parameters for vortex motion for (1) the array in the continuum limit and (2) the continuous 3D superconductor. For the continuous 3D superconductor the quantities are defined as follows:  $J_T$  is the applied transport current, the depairing current is  $J_p = \Phi_0/(3\sqrt{3}\pi\mu_0\lambda^2\xi)$ , the charge relaxation time is  $\tau_e = \epsilon/\sigma_0$ , the magnetic time is  $\tau_m = \sigma_0\mu_0\lambda^2$ , and the upper critical field is  $B_{c2}$ . For the array,  $R_e = 2R_n$  for a resistively shunted junction.

Mass	Terminal velocity	Viscosity	Decay time	Decay length
$M_V$	$\tilde{u}_x$	$\eta$	$\tau_v$	$\ell_f$
<b>2D Arrays</b>				
$\frac{\Phi_0^2 C}{2p^2}$	$\frac{pR_e I}{\Phi_0}$	$\frac{\Phi_0^2}{p^2 R_e}$	$\frac{1}{2} R_e C$	$p \frac{R_l R_{l1} C I}{2\Phi_0}$
for $M_1 \gg m_0$	$\frac{p}{\tau_{RC}} \frac{\beta_c}{2\pi} \frac{I}{I_c}$	$\frac{1}{2} \frac{M_v}{\tau_{RC}}$	$\frac{1}{2} \tau_{RC}$	$p \frac{1}{4\pi} \beta_c \frac{I}{I_c} \frac{R_{l1}}{R_l}$
<b>Continuous 3D superconductor</b>				
$\frac{\Phi_0^2 \epsilon_0 L_z}{4\pi\xi^2}$	$\frac{2\pi\xi^2 J_T}{\Phi_0 \sigma_0}$	$\frac{\Phi_0^2 \sigma_0 L_z}{2\pi\xi^2}$	$\frac{\epsilon_0}{2\sigma_0}$	$\frac{\pi\xi^2 \epsilon_0 J_T}{\Phi_0 \sigma_0^2}$
$\frac{1}{2} B_{c2} \epsilon_0 L_z$	$\frac{2}{3\sqrt{3}} \frac{\xi}{\tau_m} \frac{J_T}{J_p}$	$\frac{1}{2} \frac{M_v}{\tau_e}$	$\frac{1}{2} \tau_e$	$\xi \frac{1}{3\sqrt{3}} \frac{\tau_e}{\tau_m} \frac{J_T}{J_p}$

the driving current needed.

The third important assumption for applying our continuum model to a discrete array is that the vortex moves fast enough so that the geometry of the array does not effect its motion. Lobb *et al.*<sup>26</sup> have shown that there is an energy barrier to flux motion,  $E_B$  which is equal to about  $0.2E_J$  for a square array. Therefore, for our model to apply, the kinetic energy of the vortex must be great enough to overcome this barrier. In other words,  $M_v u_x^2 > 0.2E_J$ . This is equivalent to  $\beta_c (I/I_c)^2 > 0.4$ . For a typical value of  $I = 0.1I_c$ , this implies that  $\beta_c > 40$ . Nevertheless, flux can still flow for smaller  $\beta_c$ , because the transport current will lower the energy barrier by tilting it by an energy  $\Phi_0 I$ . This lowering of the energy barrier will mean that a depinning current will have to be exceeded before flux can flow. Indeed, the equation of motion for the position of a vortex in the presence of such barriers has the same form as the equation for the phase of a single resistively shunted junction with the shunt resistance given by  $R_e$ .<sup>27</sup> Therefore, the differential flux flow resistance above this depinning current will then be the same as the flux flow resistance found in this paper.

The fourth important assumption is that we have assumed that there is no Magnus-like force on the vortex, which tends to move the vortex in the direction of the applied current and causes a Hall effect. Although there has been no calculation of the Magnus-like force on a vortex in an array, we estimate the Hall angle by using the result for the Hall angle in the continuous superconductor. There the Hall angle is given by  $\tan \theta_H = \eta/(e\Phi_0 n_s^* d)$ . By analogy for an array we find  $\tan \theta_H = \hbar^2 \Delta R_n / (m^* p^2 R_e)$ , which for most classical arrays is negligible.

The fifth assumption is that we have ignored the effects of boundaries on the vortex motion. In the Appendix we show that the mass of the vortex can change near the boundary. However, if the array is more than a few lattice spacings wide, these effects can be neglected.

In summary, we have found the equations of motion for an array in the continuum limit. Two types of soli-

tonic solutions exists: charge solitons and flux vortices. The dynamics for charge solitons were characterized by a dispersion relation, and exhibited modes analogous to the Mooij-Schön modes in a one-dimensional superconductor. The dynamics of vortices for classical arrays were described by using the mass of the vortex. Most of this paper, then concentrated on the dynamics of vortex motion in classical arrays when there is no pinning. A phenomenological model of flux flow was presented in which the power dissipation occurs mainly on the junctions near the center of the vortex, which we called the core junctions. By considering the dissipating in the core junctions, we found a viscosity for vortex motion. This viscosity results in a flux flow resistance that is analogous to that found in the Bardeen-Stephen model for a continuous 3D superconductor. Furthermore, it was shown that the motion of vortices in an array can be nearly ballistic, and that the mean free path for vortices can be many lattice constants (and, hence, many coherence lengths). This is in contrast to a continuous superconductor, which has a mean free path of the order of a millionth of a coherence length. This means that the motion of vortices in a classical array is in a physically difference regime than the 3D superconductor. For example, in a classical array, there exist the possibility of detecting ballistic vortices.

#### ACKNOWLEDGMENTS

We would like to thank D. van der Marel, Gerd Schön, Ulrich Eckern, B.J. van Wees, P. Hadley, and F.C. Fritschy for useful discussions. T.P.O. gratefully acknowledges support from the Technical University of Delft and the National Science Foundation Grant No. DMR-8802613. J.E.M. and H.S.J.v.d.Z. acknowledge support by the Dutch Foundation for Fundamental Research on Matter (FOM).

#### APPENDIX A: MASS, ENERGY, AND FORCE OF VORTEX NEAR A BOUNDARY

The mass of the vortex is effected by the boundary and can depend on the direction of its motion with respect

to such a boundary. However, the complicating effects of the boundary will be shown to be negligible if the position of the vortex is greater than about a lattice spacing from the boundary.

Assume that the vortex in the array is confined to the semi-infinite half space for  $x > 0$  and that a bulk 3D superconductor is placed along the  $y$  axis. Let the vortex be along the  $x$  axis at the position  $x_0$ . The effect of the bulk superconductor will be modeled as making the current density near the boundary normal to the boundary. The method of images can be used to ensure this boundary condition by placing an image vortex of the same sign at the position  $-x_0$  along the  $x$  axis. The total current in the 2D superconducting region  $x > 0$  is

$$J_s(\mathbf{r}) = \frac{\Phi_0}{2\pi\mu_0\lambda_J^2} [K(|\mathbf{r} - \mathbf{r}_0|)\mathbf{i}_\phi + K(|\mathbf{r} + \mathbf{r}_0|)\mathbf{i}'_\phi], \quad (\text{A1})$$

where  $\mathbf{r}_0 = (x_0, 0)$  and the unit vectors are in the direction of the polar angles about the vortex and its image respectively. Also  $K(r)$  is the spatially distribution

$$M_v^{xx}(x_0) = M_v - \frac{C\Phi_0^2}{2\pi^2} \iint dx dy \left( \frac{1}{(x_-^2 + y^2)(x_+^2 + y^2)} - \frac{2x_0^2 y^2}{(x_-^2 + y^2)^2(x_+^2 + y^2)^2} \right), \quad (\text{A2})$$

where  $x_\pm = x \pm x_0$ . Note that the integral can be extended over all the 2D space because of the symmetry of the problem. For large distances from the boundary,  $M_v^{xx} \xrightarrow{x_0 \rightarrow \infty} M_v$  because the effect of the image is negligible. On the other hand,  $M_v^{xx} \xrightarrow{x_0 \rightarrow 0} 2\pi x_0^2 M_v / p^2 \approx 0$ , so that near the boundary this mass is zero. This can be understood because the vortex and the image create electric fields about their centers that are oppositely directed, since the image is moving in the opposite direction. Therefore, when the vortex nears the boundary the total electric field will tend to cancel out. Furthermore, for  $x_0$  about a lattice spacing, the boundary effects due to the mass are negligible.

The mass  $M_v^{yy}$  can also be found for the motion parallel to the boundary we find  $M_v^{yy} \xrightarrow{x_0 \rightarrow \infty} M_v$  and  $M_v^{yy} \xrightarrow{x_0 \rightarrow 0} 2M_v$ . Another important boundary effect is when the boundary is free-space rather than a superconductor. Then the image is of opposite sign and the func-

of the currents which is the curl of the magnetic field given in Eq. (23).<sup>19</sup> The force on the vortex, then, is the Lorentz-like force and is given by  $F_x(x_0) = \Phi_0 J'(x_0) d$ , where  $J'(x_0)$  is the sum of all the current densities from all the other vortices, evaluated at the position  $x_0$  of the vortex. By using an image vortex we find that this force can be described as the result of an interaction energy  $W_{\text{int}}$  given by  $W_{\text{int}} = -\pi E_J \ln [x_0 / (\lambda_\perp + x_0)]$ . The total energy of the vortex also includes the self-energy  $\mathcal{E}_v$  of the vortex and the energy in the 3D superconductor.

The motion of the vortex near the boundary is not only complicated by the additional potential that the vortex experiences but also by the fact that the mass of the vortex changes near the boundary. Because the electric field changes due to the boundary, the mass will also be expected to change. The phase of the wave function  $\theta$  is the sum of the phase of the vortex and its image. The calculation of the energy stored in the electric field leads to a mass  $M_v^{xx}(x_0)$  for the vortex traveling in the  $x$  direction near the boundary of

tional limiting forms of  $M_v^{xx}$  and  $M_v^{yy}$  are interchanged. In other words, for a vortex moving near a free-space boundary  $M_v^{xx}$  approaches  $2M_v$  but  $M_v^{yy}$  vanishes.

Another important boundary configuration is the vortex in an infinitely long strip of width  $b$  that it bounded by a 3D bulk superconductor. To satisfy the boundary conditions an infinite series of positive images are needed. For narrow strips such that  $b \ll \lambda_\perp$ , the corresponding interaction energy is  $W_{\text{int}}(x_0) = \pi E_J \ln \cos(\pi x_0 / b)$ .

Therefore, there is always a confining potential that ensures that the vortex is pushed back towards the center of the strip. Near the center of the strip, in fact, this confining potential is parabolic. If the vortex samples only the region near the center, then it will see only the parabolic potential and will have quantum energy levels separated by the resonant frequency of  $\omega_0 = \sqrt{\pi p} \Omega / (2b)$  so that the resonant frequency depends on the width of the confining strip.

\*Permanent address: Department of Electrical Engineering and Computer Science, Massachusetts Institute of Technology, Cambridge, MA 02139.

<sup>1</sup>Proceedings of the NATO Advanced Research Workshop on Coherence in Superconducting Networks, Delft, The Netherlands, 1987, edited by J.E. Mooij and G.B. Schön, [Physica B **152**, 1 (1988)].

<sup>2</sup>A.I. Larkin, Yu.N. Ovchinnikov, and A. Schmid, Physica B **152**, 266 (1988).

<sup>3</sup>Ulrich Eckern and Albert Schmid, Phys. Rev. B **39**, 6441

(1989).

<sup>4</sup>J.E. Mooij and Gerd Schön, Phys. Rev. Lett. **55**, 114 (1985).

<sup>5</sup>This is the same as the energy term label  $U$  in Larkin, Ovchinnikov, and Schmid (see Ref. 2).

<sup>6</sup>One could, of course, work with a two-dimensional energy density, but a three-dimensional density is used here so that the comparison with a usual three-dimensional superconductor will be more apparent.

<sup>7</sup>See Eq. (1.1) in Eckern and Schmid (see Ref. 3).

- <sup>8</sup>A.I. Larkin and Yu.N. Ovchinnikov, Phys. Rev. B **28**, 6281 (1983).
- <sup>9</sup>Ulrich Eckern, G. Schön, and V. Ambegaokar, Phys. Rev. B **30**, 6419 (1984).
- <sup>10</sup>C.J. Pethick and H. Smith, in *Nonequilibrium Superconductivity, Phonons, and Kapitza Boundaries*, edited by K.E. Gray (Plenum, New York, 1981), Chap. 15.
- <sup>11</sup>M. Tinkham, *Introduction to Superconductivity* (McGraw-Hill, New York, 1975).
- <sup>12</sup>R.P. Feynman, R.B. Leighton, and M. Sands, *The Feynman Lectures on Physics* (Addison-Wesley, Reading, MA, 1964), Vol. III, Chap. 21.
- <sup>13</sup>T.P. Orlando and K.A. Delin, *Foundations of Applied Superconductivity* (Addison-Wesley, Reading, MA, 1991). This textbook discusses in detail the merits and limitations of the MQM.
- <sup>14</sup>L.I. Schiff, *Quantum Mechanics*, 3rd ed. (McGraw-Hill, New York, 1968), p. 386.
- <sup>15</sup>W. Yourgrau and S. Mandelstam, *Variational Principles in Dynamics and Quantum Theory* (Dover, New York, 1979).
- <sup>16</sup>K.K. Likharev, N.S. Bakhvalov, G.S. Kazacha, and S.I. Serdyukova, IEEE Trans. Magn. **MAG 25**, 1436 (1989).
- <sup>17</sup>J.E. Mooij, B.J. van Wees, L.J. Geerligs, M. Peters, R. Fazio, and Gerd Schön (unpublished).
- <sup>18</sup>N.S. Bakhvalov, G.S. Kazacha, K.K. Likharev, and S.I. Serdyukova (unpublished).
- <sup>19</sup>J. Pearl, Ph.D. thesis, Polytechnic Institute of Brooklyn, New York, 1965.
- <sup>20</sup>I.O. Kulik, Fiz. Nizk. Temp. **5**, 1391 (1979).
- <sup>21</sup>K.K. Likharev, *Dynamics of Josephson Junctions and Circuits* (Gordon and Breach, New York, 1986).
- <sup>22</sup>The mass of the vortex is due to the fact that a moving vortex generates an electric field and the electromagnetic mass of this field is the vortex mass. The characteristic electrical energy in the array is the charging energy  $E_c = e^2/(2C)$ . It is interesting to note that  $M_1$  corresponds to the mass of a particle in a box of length  $p$  when the ground state of the quantum energy of that particle equals the charging energy. Likewise, for a 3D continuous superconductor the mass of a vortex of length  $L_z$  is  $M_v = \Phi_0^2 \epsilon_0 L_z / (4\pi \xi^2)$ . This is equivalent to the rest mass of a particle that has a magnetic field  $H_{c2}$  stored in the volume of the core  $L_z \pi \xi^2$ , namely,  $M_v c^2 = \mu_0 H_{c2}^2 L_z \pi \xi^2$ . It is also the mass of a particle confined to a cylinder of radius  $\xi$  such that its ground-state energy is equal to the Coulomb energy of two electrons a distance  $L_z$  apart.
- <sup>23</sup>J. Bardeen and M.J. Stephen, Phys. Rev. **140A**, 1197 (1965).
- <sup>24</sup>R. Leubwohl and M. J. Stephen, Phys. Rev. **163**, 367 (1967).
- <sup>25</sup>This assumption is similar to that used by Larkin, Ovchinnikov, and Schmid (see Ref. 2).
- <sup>26</sup>C.J. Lobb, D.W. Abraham, and M. Tinkham, Phys. Rev. B **27**, 150 (1983).
- <sup>27</sup>H.S.J. van der Zant, F.C. Fritschy, T.P. Orlando, and J.E. Mooij, Physica B **165&166**, 969 (1990).